**SUPPORTING ONLINE MATERIAL**

# 1 Materials and Methods

## 1.1 Event Characterization

The event occurred in the slab of the Santa Cruz Islands subduction zone. Depth phases pPKIKP+pPKiKP and pPKJKP are reflected from the oceanic floor, and the distances of their surface bounce points are within 12 km. This requires us to take both a magma wedge and an oceanic layer into account in the near source region. In a magma wedge, quality factors for both compressional and shear waves are thought to be extremely low (approximately 50 and 20, respectively) *(S1)*; in an oceanic layer, part of the energy of reflected phases leaks into the water. We use the moment tensor from the PDE bulletin of the National Earthquake Information Center (http://neic.usgs.gov/neis/sopar/) and the source time function (Fig. 1C) obtained from the P phase observed at YAK.

Due to the strong attenuation and poor phase conversions in the inner core, we need to select large earthquakes to search for inner core shear waves. The two events used in the last two studies *(5)(6)* are both Mw $\sim$ 8.0. However, their corresponding source durations are also much longer (approximately 20 and 40 seconds *(S2)*), and so the chance for PKJKP and pPKJKP to interfere with other phases is also higher. Thus, it is better to find an event which can balance the magnitude and the source duration. In this study, we systematically examined other large events in Tonga and Santa Cruz Islands regions. Combinations of epicentral distance, event depth, and source duration result in contamination of the potential PKJKP by other phases. We believe this is one of the important reasons why PKJKP is so difficult to observe.

## 1.2 Direct Solution Method (DSM)

So far, the identifiable phases for which we may specify the ray paths are very limited. For example, there are only $\sim$ 100 phases in the IASPEI standard seismic phase list. However,

theoretically, the number of the possible phases should be infinite. It means that most of the phases are unidentifiable because they are very weak. These phases are usually negligible, but if we want to study the elusive PKJKP phase, they might cause serious problems.

Therefore, for the synthetic modeling of PKJKP, completeness of synthetic seismograms is required. All the synthetic codes which are based on the specification of ray paths are no longer adaptable. DSM computes the displacement solution directly from the Galerkin weak form of elastic equation of motion *(S3)*. It can be used to generate highly accurate and complete synthetic seismograms *(13)*.

## 1.3 Envelope Function Modeling

Heterogeneity in the mantle can give rise to dispersion and phase shift of the waveform. Thus we choose to model the envelope function rather than directly the waveform in order to better constrain the arrival of the PKJKP phase. The envelope function is the modulus of a complex trace, for which the original trace is the real part and its Hilbert transform is the imaginary part. In general, the envelope function can characterize the amplitude and arrival time of the energy extrema better than the waveform. The synthetic vespagram for the pseudo-liquid inner core (Fig. 4A or S3A) implies that we cannot directly use the synthetic envelope function for the solid inner core to constrain the shear wave velocity. In the time window of interest (Fig. 4A or S3A), sPcPPKIKP (predicted slowness and arrival time are 1.93 s/deg and 1674 s, respectively) and pPcPPKIKP (predicted slowness and arrival time are 1.93 s/deg and 1665 s, respectively) should have appeared. But the relatively strong synthetic mantle phases (D in Fig 4A or S3A), whose slownesses are $\sim 8.0 s/deg$, arrive at the same time. The consequence is that only the dominant energy is apparent in the vespagram. Only PcPPKIKP (predicted slowness and arrival time are 1.93 s/deg and 1645 s, respectively) seems less contaminated (Fig. S3A and S3B). The synthetic phase E arrives at almost the same time as the predicted PKJKP. Therefore, it is not possible to obtain a reliable synthetic envelope function for PKJKP from the synthetic seismograms generated for a solid inner core.

The absence of the mantle phase E (Fig. S3A) in the observed vespagram suggests that we can directly use the envelope function of PKJKP in the synthetic differential seismogram between the solid inner core and the 'pseudo-liquid' inner core, where the mantle phase E is removed, to constrain the shear wave velocity and $Q_\beta$ (this will be addressed in a separate publication) in the inner core.

### 1.4 Potential Interfering Phases in the PKJKP Window

In the epicentral distance range ($\sim 138^o$) of our study, theoretically, four phases (PcPPKIKP, pPcPPKIKP, sPcPPKIKP, and PKKPdf) (Fig. 3) could be present in our PKJKP windows (Fig. 2C and D; Fig. 4A and B) with respect to the reference seismic model PREM *(7)*. Nevertheless, few of PKKPdf have been observed due to its very small reflection coefficient at the CMB *(S4)*. On the other hand, predicted PcPPKIKP and its two depth phases are barely starting to exist at the distance of GRF (Fig. S4). Thus, their observabilities are strongly dependent on the heterogeneity of the real earth.

## 2 Supporting References


S1. M. Barazangi, B. Isacks, *J. Geophys. Res.* **76**, 8493 (1971).

S2. S. Goes, L. Ruff, N. Winslow, *Geophys. Res. Lett.* **24**, 1295 (1997).

S3. R.J. Geller, T. Ohminato, *Geophys. J. Int.* **116**, 421 (1994).

S4. P.S. Earle, P.M. Shearer, *Science* **277**, 670 (1997).


## 3 Supporting Figures

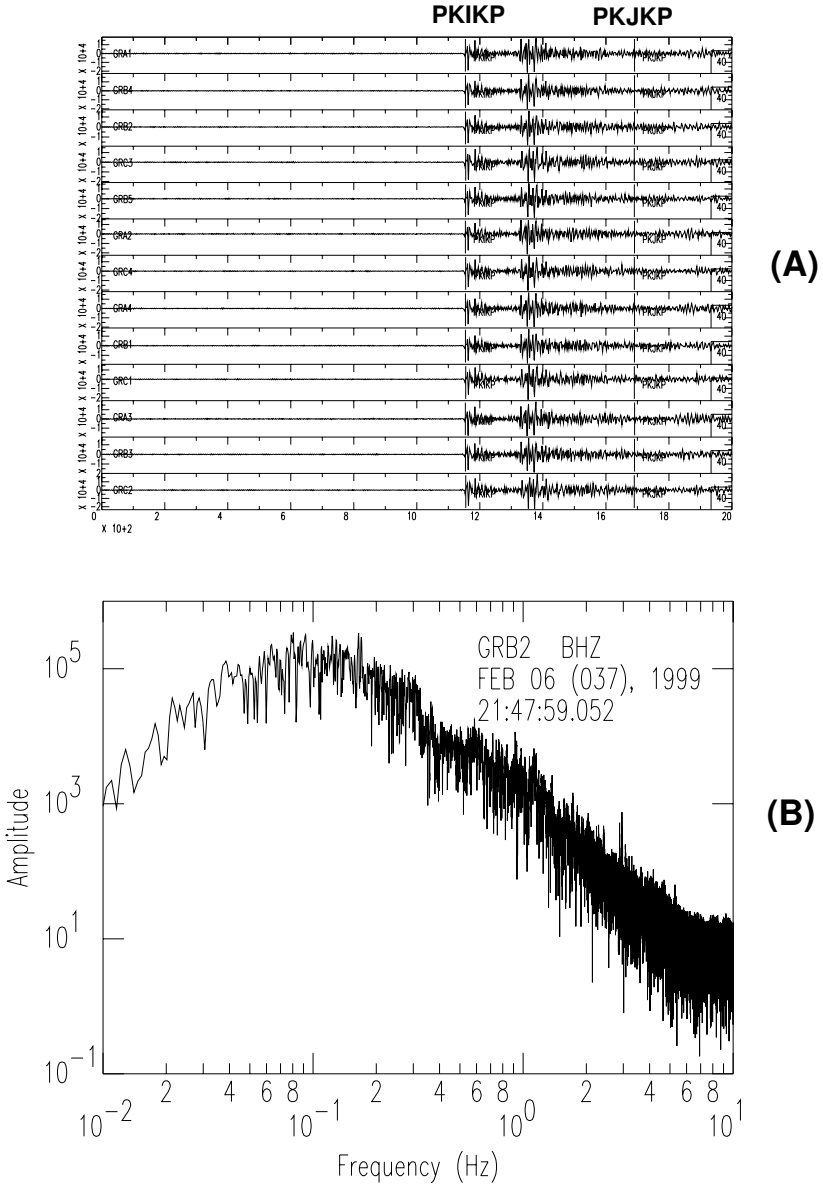


Figure S1: (A) Vertical component raw traces for the 02/06/1999 Santa Cruz Island event, starting at the origin time, for stations of the GRF array. PKIKP and PKJKP phases are labeled, respectively. PKJKP is not visible in the individual traces. We choose station GRB2, which is at the center of the GRF array, as the reference station. (B) An example of amplitude spectrum. The time window used to compute the spectrum is from 100 seconds before PKIKP to 200 seconds after PKJKP. The amplitude spectrum is maximum and relatively constant in the frequency range 0.06 to 0.1 Hz.

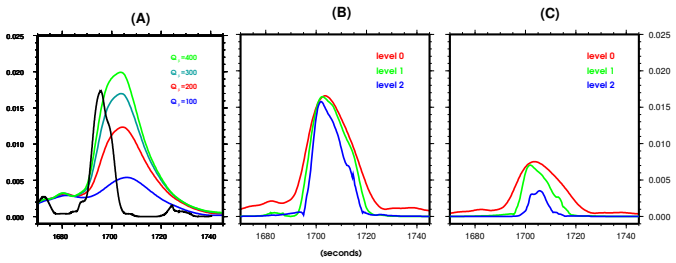


Figure S2: (A) Envelope function modeling. The solid black line corresponds to the observed PKJKP, and color lines indicate synthetic PKJKP for different shear wave quality factors assumed in the inner core. Note that a $Q_\beta \sim 300$ appears to fit the data best. Further investigation of this measurment is underway. The envelope function of the observed PKJKP is narrower than that of the synthetic PKJKP. This is due to the background noise at the GRF stations. The existence of the incoherent noise can make the waveform narrower after non-linear stacking *(13)*. (B) and (C) are the background noise experiments. The original amplitude in panel (B) is $\sim 2.2$ times larger than in panel (C). The results indicate that adding background noise (using 200 to 300 s before the first arrival) at individual stations into the synthetic differential seismograms can narrow the resulting envelope functions, as well as reduce the amplitudes. Level 0: no seismic noise is added to synthetic PKJKP traces; Level 1: the original strength of seismic noise is added, and the corresponding amplitude ratio increases to $\sim 2.4$; Level 2: the strength of seismic noise is amplified twice before being added to the individual traces, and the corresponding amplitude ratio increases to $\sim 4.8$. The results show that the lower the original amplitude, the more influenced by the background noise after stacking.

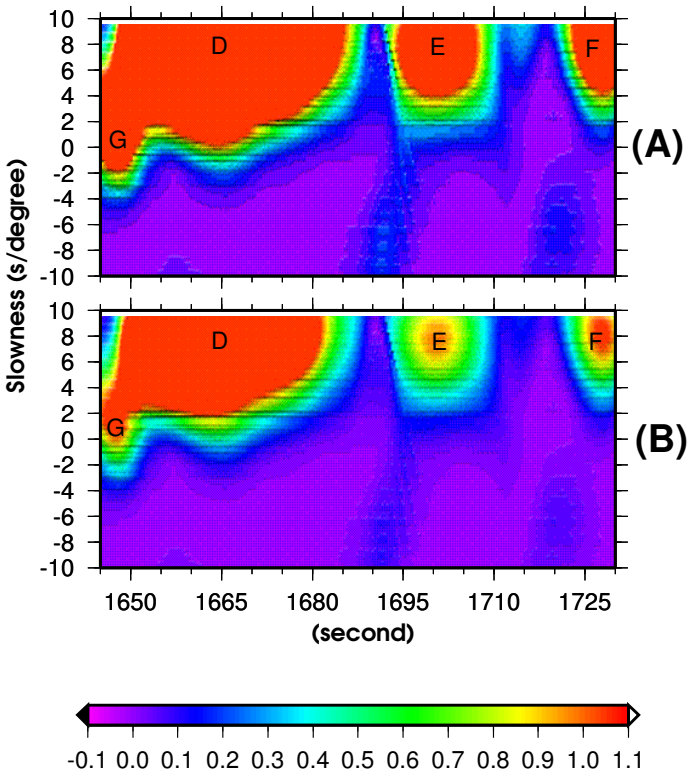


Figure S3: Synthetic vespagrams in the slowness and travel time domain. (A) for the pseudo-liquid inner core, which is the same as Figure 4A. (B) Same as (A), but energy level is amplified 20 times, to bring out the relative strengths of these phases. By comparing the synthetic vespagram (Fig. S3A) with the observed vespagram (Fig. 2C), we may note that mantle phases E and F (Fig. S3A) are not observed in the real earth. Only the mantle phase D, which is stronger than mantle phases E and F (Fig. S3B), remains in the observed vespagram. This is most likely due to seismic scattering caused by mantle heterogeneity.

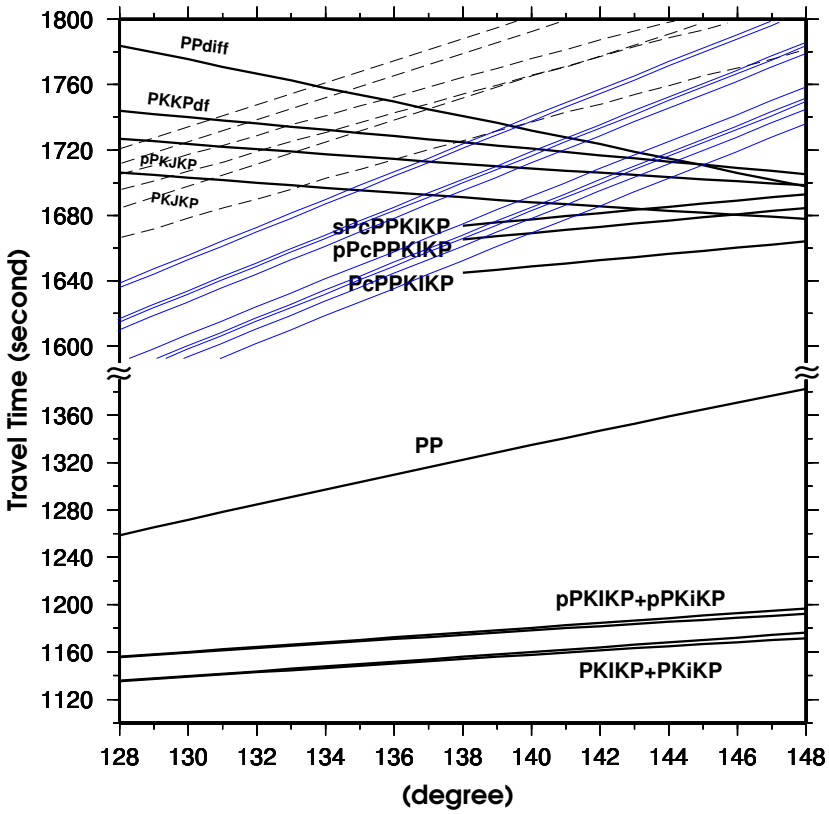


Figure S4: travel times of the phases related to this study (with respect to PREM model). The epicentral distance range of study is $\sim 138^o$. The thin dashed lines are the travel time curves of SKKS, SKKKS, pSKKS, sSKKS, pSKKKS, and sSKKKS phases, respectively, along the travel time axis on the left. The thin blue lines are the travel time curves of pPPPPPmP, pPPPP2(PmP), sPPPPPmP, pPPPP3(PmP), sPPPP2(PmP), sPPPP3(PmP), sPPPP6(PmP), pPPPP8(PmP), sPPPP7(PmP), pPPPP11(PmP), and sPPPP10(PmP), respectively, where n(PmP) means the wave is reflected n times at the Moho. In terms of the travel times and slownesses, the mantle phase D in Fig. 4 matches pPPPPPmP, pPPPP2(PmP), sPPPPPmP, pPPPP3(PmP), sPPPP2(PmP), and sPPP3(PmP); E matches sPPPP6(PmP), pPPPP8(PmP), and sPPPP7(PmP); and F matches sPPPP10(PmP), and pPPPP11(PmP).